Article

Cell Reports

Nrf2 Induces IL-17D to Mediate Tumor and Virus Surveillance

Graphical Abstract

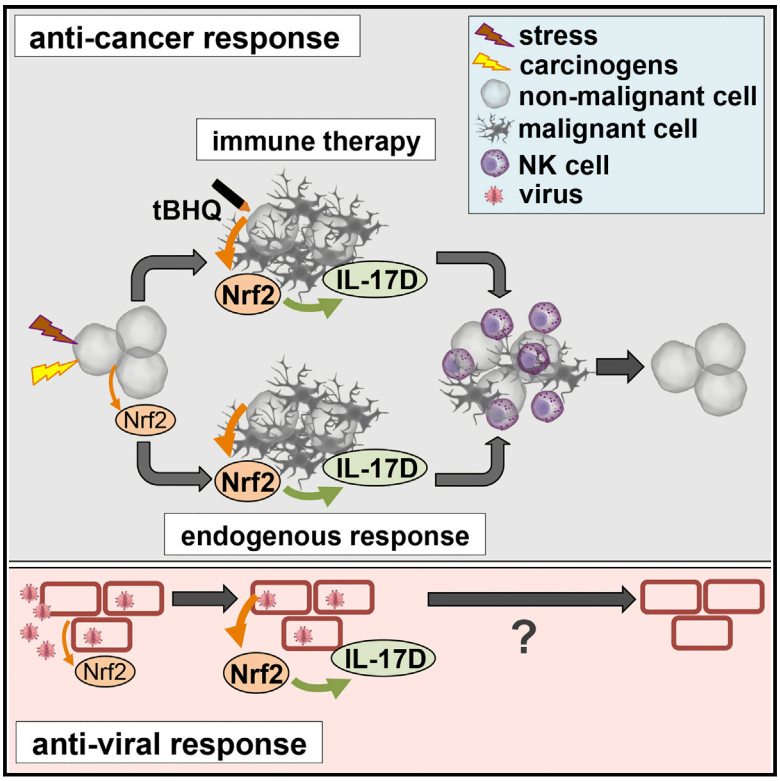

Highlights

- The transcription factor Nrf2 induces the cytokine IL-17D
- IL-17D is required for effective antitumor and antiviral immune responses
- Induction of Nrf2 by agonists in established tumors can lead to tumor regression
- IL-17D-mediated tumor regression requires Nrf2 expression in tumors

Authors

Robert Saddawi-Konefka, Ruth Seelige, Emilie T.E. Gross, ..., Timothy E. O'Sullivan, Olivier Harismendy, Jack D. Bui

Correspondence

jbui@ucsd.edu

In Brief

Saddawi-Konefka et al. show that the transcription factor nuclear factor erythroid-derived 2-like 2, or Nrf2, induces the cytokine interleukin-17D. Nrf2/IL-17D-mediated natural killer cell recruitment can lead to the regression of established tumors. Therefore, inducing IL-17D using Nrf2 agonists has potential for cancer immune therapy.

Saddawi-Konefka et al., 2016, Cell Reports *16*, 2348–2358
August 30, 2016
http://dx.doi.org/10.1016/j.celrep.2016.07.075

OPEN ACCESS
CellPress

Cell Reports
Article

Nrf2 Induces IL-17D to Mediate Tumor and Virus Surveillance

Robert Saddawi-Konefka,[1,4] Ruth Seelige,[1,4] Emilie T.E. Gross,[1] Eric Levy,[2] Stephen C. Searles,[1] Allen Washington, Jr.,[1] Endi K. Santosa,[1] Beichen Liu,[1] Timothy E. O'Sullivan,[3] Olivier Harismendy,[2] and Jack D. Bui[1,5,*]

[1]Department of Pathology, University of California, San Diego, San Diego, CA 92093, USA
[2]Moores Cancer Center Oncogenomics Laboratory, University of California, San Diego, San Diego, CA 92093, USA
[3]Immunology Program, Memorial Sloan-Kettering Cancer Center, New York, NY 10065, USA
[4]Co-first author
[5]Lead Contact
*Correspondence: jbui@ucsd.edu
http://dx.doi.org/10.1016/j.celrep.2016.07.075

SUMMARY

Cells undergoing xenobiotic or oxidative stress activate the transcription factor nuclear factor erythroid-derived 2-like 2 (Nrf2), which initiates an intrinsic "stress surveillance" pathway. We recently found that the cytokine IL-17D effects a form of extrinsic stress surveillance by inducing antitumor immunity, but how IL-17D is regulated remains unknown. Here, we show that Nrf2 induced IL-17D in cancer cell lines. Moreover, both Nrf2 and IL-17D were induced in primary tumors as well as during viral infection in vivo. Expression of IL-17D in tumors and virally infected cells is essential for optimal protection of the host as *il17d*$^{-/-}$ mice experienced a higher incidence of tumors and exacerbated viral infections compared to wild-type (WT) animals. Moreover, activating Nrf2 to induce IL-17D in established tumors led to natural killer cell-dependent tumor regression. These data demonstrate that Nrf2 can initiate both intrinsic and extrinsic stress surveillance pathways and highlight the use of Nrf2 agonists as immune therapies for cancer and infection.

INTRODUCTION

Cells undergoing malignant transformation or viral infection constitute cells in a "stressed state," characterized by altered metabolism and imbalanced reactive oxidative species (ROS) (Gorrini et al., 2013; Martindale and Holbrook, 2002; Schwarz, 1996). In order to deal with ROS, cells activate the transcription factor nuclear factor erythroid-derived 2-like 2 or Nfe2l2 (Nrf2). Nrf2 is a member of the cap "n" collar family of bZip transcription factors and is recognized as the primary responder to cellular oxidative stress (Ma, 2013). Nrf2 induces genes involved primarily in antioxidant defense, oxidant signaling, and drug metabolism, and secondarily, in metabolism, cell proliferation, and proteasome activity (Malhotra et al., 2010; Schäfer et al., 2012; Türei et al., 2013).

The cell-protective pathways induced by Nrf2 can have opposing effects on cancer development. For example, Nrf2 protects somatic and premalignant cells from carcinogens and, in this context, fulfills a tumor suppressor role (Kensler and Wakabayashi, 2010; Ma and He, 2012). On the other hand, it is well-documented that Nrf2 can promote the growth and survival of established tumors by inducing anti-oxidative pathways that help cancers deal with chronic oxidative stress, a hallmark of cancer progression (Jaramillo and Zhang, 2013; Sporn and Liby, 2012). It is not known whether Nrf2 regulates extrinsic stress response mechanisms that operate to suppress carcinogenesis.

Recently, our group identified the cytokine IL-17D as a molecule expressed at higher levels in highly immunogenic tumor cells compared to poorly immunogenic tumor cells (O'Sullivan et al., 2014; Saddawi-Konefka et al., 2015). When IL-17D was overexpressed in poorly immunogenic cancer cells, it led to immune rejection mediated by natural killer (NK) cells. The regulation of IL-17D is not known, but based on its tumor rejection activities, we hypothesize that IL-17D would initiate tumor surveillance and thus accompany early cellular transformation.

Here, we show direct and compelling evidence that Nrf2 induces the expression of IL-17D, therefore initiating antitumor immune responses. We also find that viral infection induces Nrf2 and IL-17D, presumably by causing local oxidative stress. The induction of IL-17D is required for effective cancer surveillance and antiviral responses, as mice deficient in IL-17D had increased formation of MCA-induced tumors and exacerbated pathology when infected with vaccinia virus (VV) or murine cytomegalovirus (MCMV). Our data document a link between cellular oxidative stress—resulting from viral infection or tumorigenesis—and the initiation of immunity. Moreover, our results define an immune activating role for the well-studied factor Nrf2, which has not been previously defined. This role for Nrf2 in inducing IL-17D has therapeutic benefit in our mouse models.

RESULTS

Nrf2 Induces IL-17D

To explore IL-17D regulation, we performed a transcription factor binding site (TFBS) analysis of the promoter and intronic regions of the human and mouse *il17d* genes (Figure 1A). Our

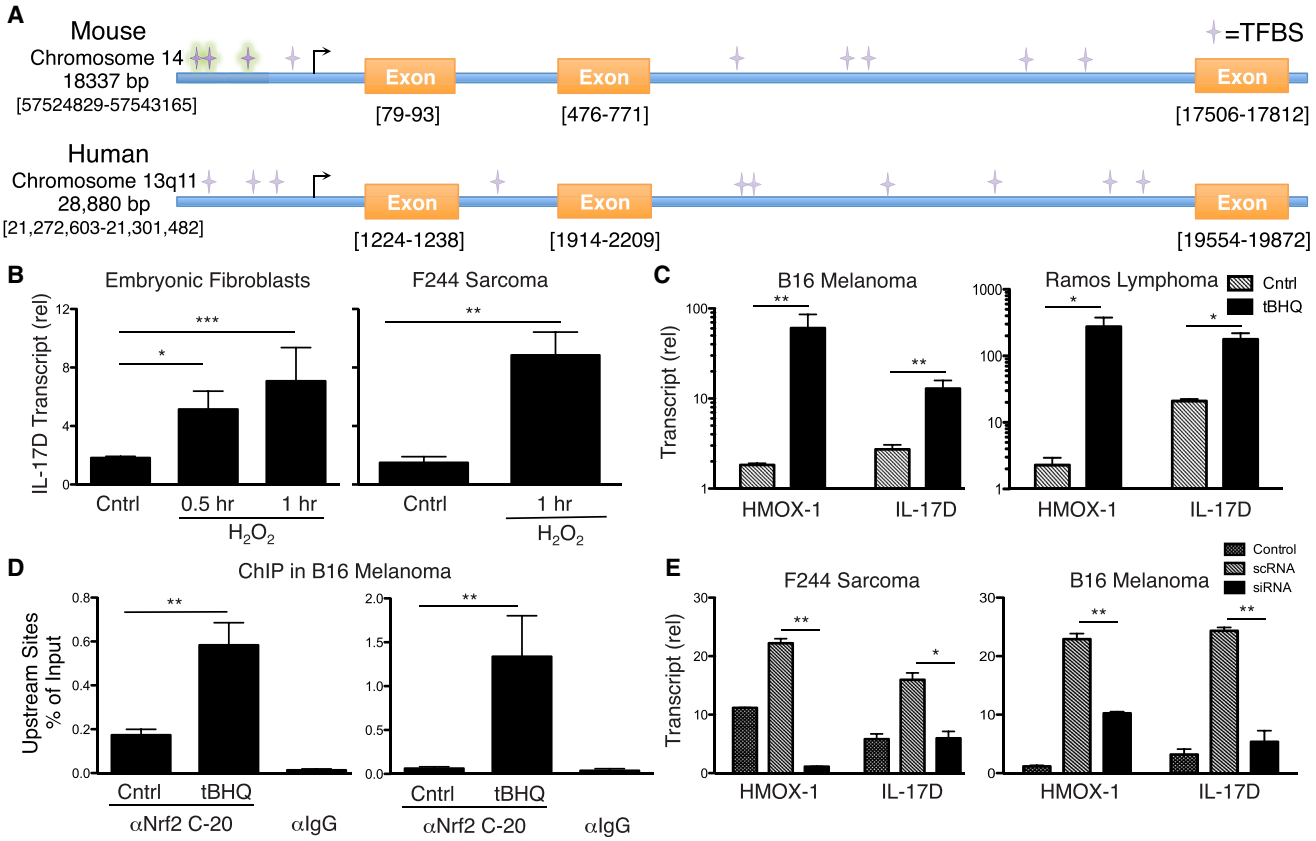

Figure 1. The Transcription Factor Nrf2 Induces IL-17D

(A) Consensus sequence analysis of Nrf2 TFBS in the promoter and intronic regions of human and mouse *il17d* genes. Green highlights represent Nrf2 binding sites in (D).

(B) H_2O_2 activates Nrf2 and induces *il17d* in MEFs (left) and MCA-induced sarcoma (right).

(C) Pharmacologic activation of Nrf2 with tBHQ induces *il17d* in the murine melanoma B16 (left) and human Burkitt's lymphoma cell line Ramos (right).

(D) ChIP of B16 melanoma cells treated with tBHQ shows that Nrf2 directly binds to chromatin upstream of the *il17d* gene (regions around 4196, 4860 (left), and 3730 bp (right) upstream of the *il17d* start site). Values are expressed as the % of Nrf2 bound in immunoprecipitated samples compared to input samples.

(E) siRNA to *nrf2* prior to activation with H_2O_2/tBHQ in tumor cell lines blocks the induction of *il17d* in MCA sarcoma (left) or B16 melanoma (right). TFBS, transcription factor binding site.

Experiments repeated at least twice. Error bars represent ± SEM. See also Figure S1 and Tables S1 and S3.

analysis revealed several putative Nrf2 binding sites, defined as anti-oxidant responsive elements (ARE) (Nguyen et al., 2003) (Figure 1A; Table S1). Given the abundance of ARE in promoter and intronic regions of *il17d*, we hypothesized that the activation of Nrf2 would induce IL-17D. To test this, we treated murine embryonic fibroblasts (MEFs) and the 3-methylcholanthrene (MCA)-induced sarcoma cell line F244 (O'Sullivan et al., 2012; Shankaran et al., 2001) with H_2O_2, a known activator of Nrf2 (Pergola et al., 2011; Tkachev et al., 2011) (Figure 1B). H_2O_2 treatment led to significant, time-responsive increases in the transcript of *il17d*. Similarly, activation of Nrf2 with *tert*-butylhydroquinone (tBHQ) resulted in the increase of *il17d* transcript in the murine melanoma cell line B16, the human Burkitt's lymphoma cell line Ramos, and in the MCA-induced sarcoma cell line F244 (Figures 1C and S1A).

Next, we determined whether the transcription factor Nrf2 directly binds to the TFBS we identified in our analysis of the *il17d* gene. We performed a chromatin immunoprecipitation followed by PCR amplification of specific sequences (ChIP-qPCR) in tBHQ-treated or control-treated B16 cell lines. Cells were fixed and sonicated before immunoprecipitation with Nrf2-specific antibody or control IgG. Fractionation and western blot analysis confirmed that Nrf2 preferentially accumulated in the nuclear fraction of treated cells (not shown). qPCR analysis of ChIP fractions revealed two sites upstream of the *il17d* start site where Nrf2 has significant binding following activation (Figure 1D). These two binding sites for Nrf2 corresponded to Nrf2 target ARE elements identified at 4195, 4860, and 3730 bp upstream of the *il17d* start site (Figure 1A; Table S1). qPCR analysis of the known gene target for Nrf2, heme oxygenase 1 (*hmox1)*, also indicated Nrf2 binding following tBHQ treatment in the B16 cell line (Figure S1B).

TFBS analysis with the ENCODE UCSC browser revealed that other transcription factors might bind and regulate IL-17D (data not shown), indicating that Nrf2 may not be wholly responsible for the induction of IL-17D. In order to examine the necessity of

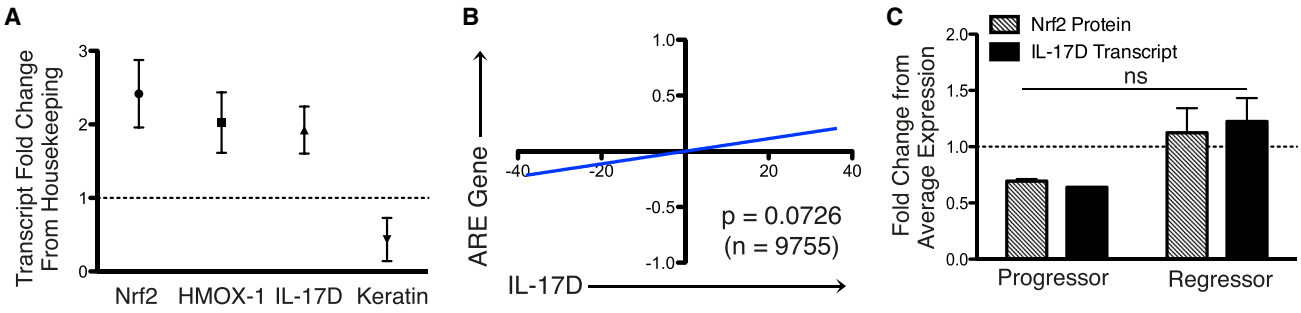

Figure 2. Nrf2 Is Activated in Primary Murine Tumors, and Its Activation Correlates with the Expression of *il17d* in Human Cancers

(A) Expression of *nrf2*, *hmox1*, *il17d*, and *keratin* in primary MCA-induced sarcomas (n = 9) assessed via qPCR and compared to normal untreated skin (n = 6).

(B) Expression of *il17d* in all available TCGA human cancers correlates with the expression of ARE-containing genes.

(C) MCA-induced sarcomas grouped according to their growth phenotype in WT mice (n = 3 per group) show correlations in their expression of *il17d* transcript and Nrf2 protein.

Experiments repeated at least twice. Error bars represent ± SEM. See also Figure S2.

Nrf2 for the induction of IL-17D, we activated Nrf2 in the F244 or B16 cell lines in the presence of siRNA specific to *nrf2* (Figures 1E, S1C, and S1D) and in F244 and B16 cell lines bearing a stable knockdown of *nrf2* via small hairpin RNA (shRNA) (Figures S1E–S1J). Knockdown of Nrf2 in B16 and F244 (~80%, Figures S1C–S1F) was sufficient to block the induction of *il17d* following activation of Nrf2 with either H_2O_2 or tBHQ. Altogether, we found that Nrf2 not only directly bound to the *il17d* promoter region but also was required for efficient induction of *il17d* by oxidative stress.

Nrf2 and IL-17D Are Co-expressed in Primary Tumors and during Viral Infection

To determine the relevance of the Nrf2 regulation of IL-17D in vivo, we examined the expression of IL-17D, Nrf2, and its known target genes in primary human and mouse tumors. Analyzing gene expression in primary MCA-induced tumors (from Figure 4A) revealed that *nrf2*, its target *hmox1*, and *il17d* were upregulated compared to normal untreated skin samples (Figure 2A). Using data sourced from The Cancer Genome Atlas (TCGA), we found that *il17d* expression directly correlated with the expression of ARE-containing Nrf2 targets (signature of nine genes in total, see the Experimental Procedures) across all available human cancers (n = 9,755) (Figure 2B). The results are not significant (p = 0.07), likely due to the fact that TCGA data include many tumors harvested at late time points, when we hypothesize *il17d* and *nrf2* expression to be uncoupled due to editing of IL-17D (O'Sullivan et al., 2014). Moreover, infiltrated immune cells that have a different gene expression profile can influence the results (Aran et al., 2015). We also found that a high level of IL-17D expression in 13 out of 31 human cancer types confers a survival advantage (Table S2), representatively shown for brain lower grade glioma and ovarian serous cystadenocarcinoma (Figure S2A). Additionally, an analysis of our MCA-sarcoma tumor cell lines demonstrated that Nrf2 and *il17d* are co-expressed in murine tumor cell lines (Figure 2C). Matching our previous data (O'Sullivan et al., 2014; Saddawi-Konefka et al., 2015), cell lines expressing high levels of IL-17D tended to behave as regressors, now underlined by their co-expression of Nrf2. Together, these data suggest that Nrf2 regulates IL-17D during primary tumor formation in both human and mouse systems in order to initiate productive antitumor immune responses leading to tumor regression and prolonged survival. IL-17D expression only correlates with better survival in a fraction of human cancers (Figure S2; Table S2), suggesting that its regulation might be context-dependent and underlining the importance of analyzing its regulation in defined in vivo mouse models.

Viral infections represent another sort of cellular stress. Because IL-17D recruits NK cells that can mediate antiviral responses, we sought to examine the role of the Nrf2-IL-17D axis in antiviral immunity. First, we measured Nrf2 and IL-17D following vaccinia virus (VV) and murine cytomegalovirus (MCMV) infection. In vitro, we observed an increase in the transcript levels of *il17d* in both infected primary-derived fibroblasts and tumor cell lines (Figures 3A and 3B). The results in the tumor cell lines are not significant, likely due to the fact that tumors are not the primary target for viruses. For in vivo analysis, we scarified WT mice with VV. Tissue harvested from these mice had increased expression of *il17d* and Nrf2 (Figures 3C and 3D; see Figures S3A and S3B for an example of VV scar). To model the local activation of Nrf2 and IL-17D in vivo, we adapted a system in which we topically applied tBHQ onto the dorsal flanks of mice (Schäfer et al., 2014). Mice treated topically with tBHQ had increased transcript and protein levels of *il17d* and Nrf2, respectively, commensurate with those observed following infection by scarification (Figures 3E and 3F). Together, these results suggest that the Nrf2-IL-17D regulatory axis is activated during primary tumorigenesis and viral infection in order to confer protection from disease progression.

IL-17D Protects the Host from Primary Tumorigenesis and Viral Infection

We previously showed that IL-17D can mediate tumor rejection when overexpressed in cancer cells (O'Sullivan et al., 2014), but its endogenous role in cancer immunosurveillance had not been demonstrated. Therefore, we compared the development of primary tumors in WT versus *il17d*$^{-/-}$ mice, each treated with the carcinogen 3-methylcholanthrene (MCA). Because the immune cellularity of *il17d*$^{-/-}$ mice has not been studied, we first immune-phenotyped these mice. We found that the major

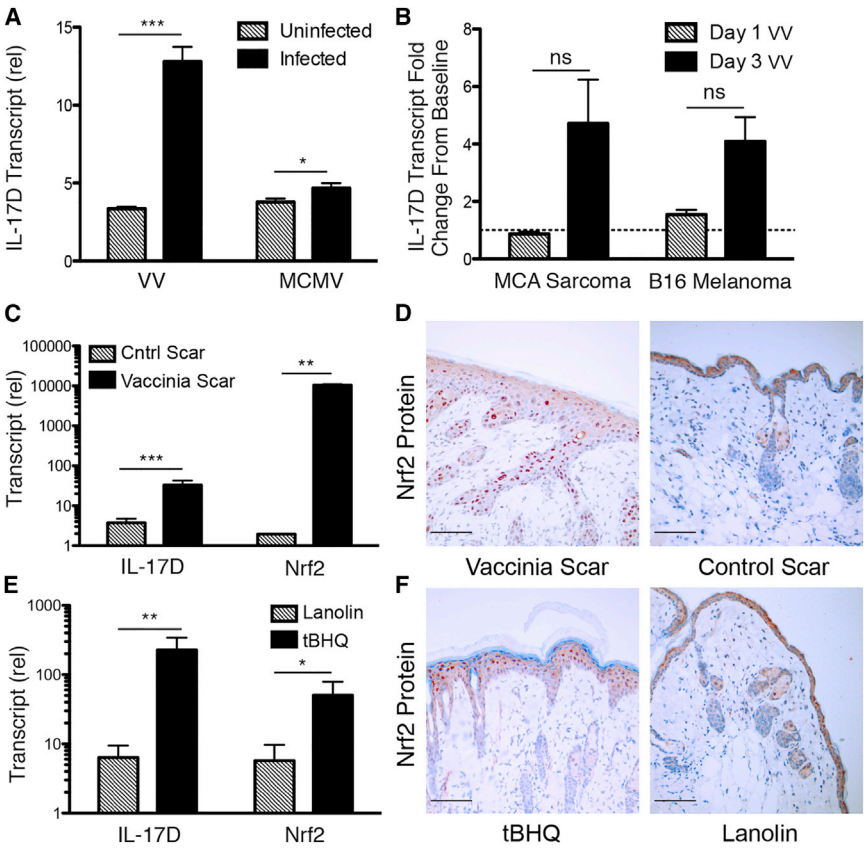

Figure 3. The Expressions of *il17d* and Nrf2 Correlate following Viral Infection

(A) Primary-derived adult fibroblasts infected with vaccina virus (VV) or mouse cytomegalovirus (MCMV) show an increase in the transcript of *il17d*.

(B) An MCA sarcoma or B16 melanoma cell line increases *il17d* transcript following VV infection in vitro.

(C) Infection by scarification with VV in vivo leads to an increase in *il17d* and *nrf2* transcript expression.

(D) IHC for Nrf2 protein in infected versus non-infected scars show an increase in Nrf2 protein expression in skin spanning dermis to epidermis. Scale bar, 200 μm.

(E) Topical application of tBHQ on the flank in vivo increases *il17d* and *nrf2* transcript expression.

(F) Nrf2 protein expression is similarly increased following tBHQ topical applications.

Experiments repeated at least twice. Error bars represent ± SEM. See also Figure S3.

immune populations in the spleen, lymph node, bone marrow, and blood were similar between WT and *il17d*$^{-/-}$ mice (Figure S4 and data not shown). Despite demonstrating a largely normal immune system at baseline, strikingly, *il17d*$^{-/-}$ mice were significantly more susceptible to the development of primary tumors (Figure 4A). At a 25-μg dose of MCA, approximately twice the number of *il17d*$^{-/-}$ mice compared to WT mice developed primary tumors. At a 5-μg dose of MCA, WT mice are largely tumor-free, whereas ~40% of *il17d*$^{-/-}$ mice developed primary tumors. These findings confirm that, similar to Nrf2, the cytokine IL-17D can protect the host from primary carcinogen-induced tumor formation.

Because we found Nrf2 and IL-17D to be induced after viral infection, we next tested the role of IL-17D in viral infection. Following infection of WT and *il17d*$^{-/-}$ animals, we observed an exacerbation of the VV scar in *il17d*$^{-/-}$ animals compared to WT animals at two doses (Figure 4B). Similarly, *il17d*$^{-/-}$ mice were more susceptible to another virus, MCMV, displayed as an increase in weight loss after systemic infection (Figure 4C). To test whether IL-17D can directly inhibit viral replication or progression, we infected either parent or IL-17D-expressing tumor cell lines with VV (Figure S3C). Expression of IL-17D in vitro did not protect cells from infection, suggesting that IL-17D's role in protecting the host from viral infection may require the immune system. These findings imply that virus infection may activate the Nrf2-IL-17D axis to initiate surveillance and contribute to host antiviral defense.

Activating Tumor-Intrinsic Nrf2 Delays Tumor Growth In Vivo via Induction of Tumor-Derived IL-17D

Having shown a requirement for IL-17D in effective tumor surveillance (O'Sullivan et al., 2014; Saddawi-Konefka et al., 2015) (Figure 4A), we hypothesized that activating Nrf2 in vivo would induce IL-17D in established tumors, which in turn would initiate protective immunosurveillance. To examine this, tumor-bearing mice were treated topically with tBHQ or lanolin control cream beginning when tumors achieved an average diameter of 3 mm. We found that treatment with tBHQ delayed tumor growth in WT mice bearing F244 or B16 tumors (Figures 5A and 5B). Moreover, tBHQ led to the in vivo induction of both *hmox1* and *il17d* in tumors derived from both transplanted cell lines (Figure 5C).

Recognizing that tBHQ could induce Nrf2 in both host and tumor cells and that Nrf2 might induce targets other than IL-17D, we wanted to examine: first, whether tBHQ is activating Nrf2 and IL-17D in tumor cells versus host cells; second, whether tBHQ necessarily and specifically induces IL-17D to mediate tumor regression; and third, whether Nrf2 is required to induce IL-17D and delay tumor growth. Therefore, we transplanted *nrf2*$^{-/-}$ and *il17d*$^{-/-}$ mice with B16 and treated with tBHQ. We observed delayed tumor growth of B16 in *nrf2*$^{-/-}$ and *il17d*$^{-/-}$ mice (Figures 5D and 5E), demonstrating that host expression of *nrf2* or *il17d* is not required for the response to tBHQ.

To examine the role of tumor-derived IL-17D during tBHQ-induced tumor rejection, we utilized an MCA sarcoma cell line that we generated from an *il17d*$^{-/-}$ host (named F38K1; derived from the MCA experiment in Figure 4A). Based on established definitions for tumor growth phenotypes (O'Sullivan et al., 2012), we classified F38K1 as a progressor tumor (Figure S5A). We confirmed F38K1's sensitivity to Nrf2 activation by stimulating the cell line in vitro and measuring *hmox1* transcript expression, which increased in the presence of tBHQ

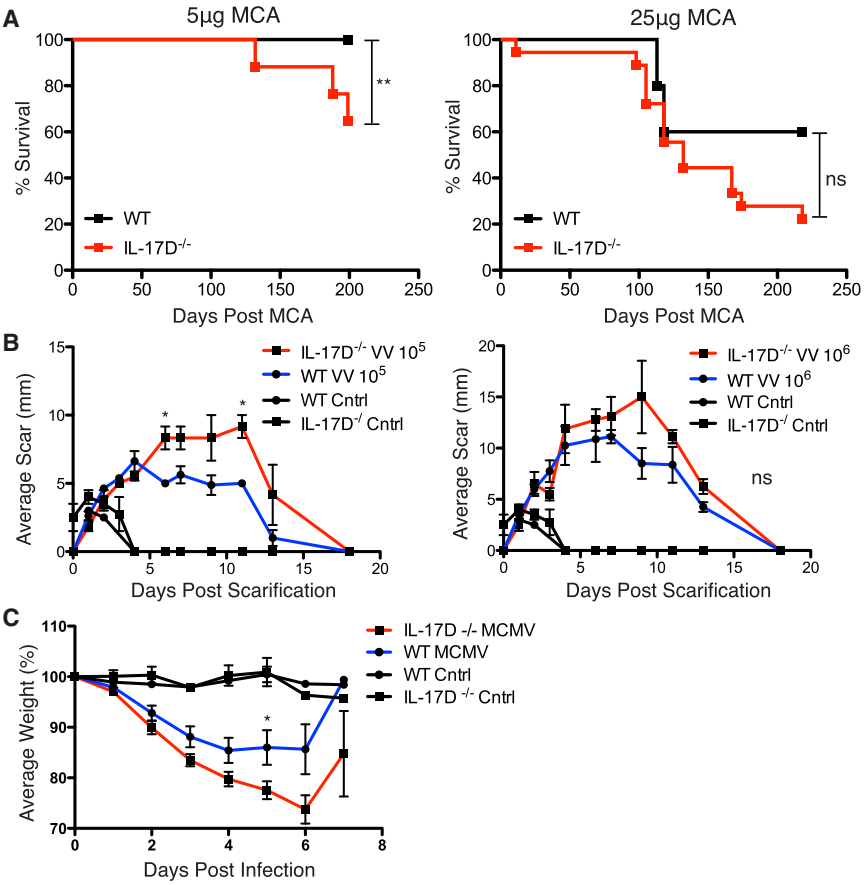

Figure 4. IL-17D Protects from Primary Tumorigenesis and Viral Infection

(A) Primary tumors induced with the carcinogen 3-MCA in *il17d*$^{-/-}$ versus WT mice develop tumors at a higher frequency at low (5 μg, left) and high doses (25 μg, right) of carcinogen.

(B) Scars infected with VV in *il17d*$^{-/-}$ mice are larger than in WT before scar resolution at both a lower ($10^{\wedge}5$, left) and higher pfu ($10^{\wedge}6$, right).

(C) *Il17d*$^{-/-}$ mice i.p. infected with 3 × 10^5 pfu MCMV are more susceptible than WT mice, as measured by weight loss.

Experiments repeated at least twice. Error bars represent ± SEM. See also Figures S3 and S4.

(Figure S5B). In vivo, tBHQ treatment in WT (Figure 5F) and *il17d*$^{-/-}$ (Figure S5C) mice transplanted with F38K1 failed to delay tumor growth. This finding implies that the antitumor response resulting from the activation of Nrf2, via topical application of tBHQ, requires tumor-expressed IL-17D and not the many previously described targets of Nrf2 (Malhotra et al., 2010; Türei et al., 2013).

To analyze the requirement of tumor-derived Nrf2 during tBHQ-induced tumor rejection, we generated independent sarcoma and melanoma cell lines bearing a stable knockdown of *nrf2* via shRNA (Figures S1E–S1J). We chose the two shRNA constructs that showed the best downregulation of *nrf2* (90% and 83% for F244 sarcoma; 88% and 80% for B16 melanoma) for further experiments. tBHQ treatment had no influence on in vitro cell growth in any of the transduced cell lines (Figures S5D and S5E and not shown). When transplanted into WT mice, tBHQ treatment failed to delay tumor growth of the two *nrf2* knockdown cell lines (Figures 5G and 5H and data not shown), in contrast to the shRNA control cell lines (Figure S5F). Moreover, the tBHQ-mediated induction of *il17d* (and *hmox1*) was abolished in vivo when *nrf2* was knocked down (Figure 5I). These results show that tumor-derived Nrf2 is required for both the tBHQ-dependent induction of *il17d* as well as the rejection of established tumors. It should be noted that silencing *nrf2* in these progressor tumors actually caused them to display growth delay compared to the parental cells (Figures 5G and 5H and not shown). These results indicate that Nrf2 may have tumor promoting activity and thus, the tumor rejection by tBHQ-induction of IL-17D must be stronger than the tumor promoting activity of Nrf2.

Activating Nrf2 Mediates Tumor Rejection via Recruitment of NK Cells

To determine whether the immune system was required for the antitumor effect of Nrf2 agonists, we transplanted B16 melanoma cells into immune-deficient mice: *rag2*$^{-/-}$, which lack adaptive immunity but possess intact NK cells and macrophages (Shinkai et al., 1992) and *rag2*$^{-/-}$ $\gamma c^{-/-}$, which lack adaptive immunity as well as NK cells (Mazurier et al., 1999). Notably, we found that topical treatment of tumors with tBHQ delayed tumor growth in *rag2*$^{-/-}$ but not *rag2*$^{-/-}$ $\gamma c^{-/-}$ (Figures 6A and 6B). This suggests that NK cells are the immune population responsible for tBHQ-mediated tumor rejection. To identify the immune cells recruited by tBHQ treatment, we harvested B16 tumors after 7 days of treatment (representative image shown in Figure 5A) and performed a fluorescence-activated cell sorting (FACS) analysis of tumor infiltrating leukocytes (TILs). Our TIL analysis revealed an increase in the percentage and total number of infiltrating NK cells when tumors were treated with tBHQ (Figures 6C–6E), a result consistent with our prior study showing that IL-17D recruited NK cells via induction of the chemokine CCL2 (O'Sullivan et al., 2014; Saddawi-Konefka et al., 2015). No other TIL populations were found to be different in treated versus untreated tumors (Figure 6C). We next investigated the requirement of Nrf2 and IL-17D for the recruitment of NK cells. When *nrf2* was knocked down or *il17d* was deleted within the tumor cell (by transplanting the cell line F38K1), the tBHQ-mediated increase in NK cells was abolished (Figure 6F). NK cells in tumors did not differ in activation or function (as assessed by expression of CD69, IFNγ, and Granzyme B) (Figure S5G). Together, our results show that NK cells are recruited into tBHQ-treated tumors and that tumor-expressed Nrf2 and IL-17D are required for the tBHQ-mediated recruitment of NK cells. In order to assess if *il17d* expression correlated with NK cell infiltration in human

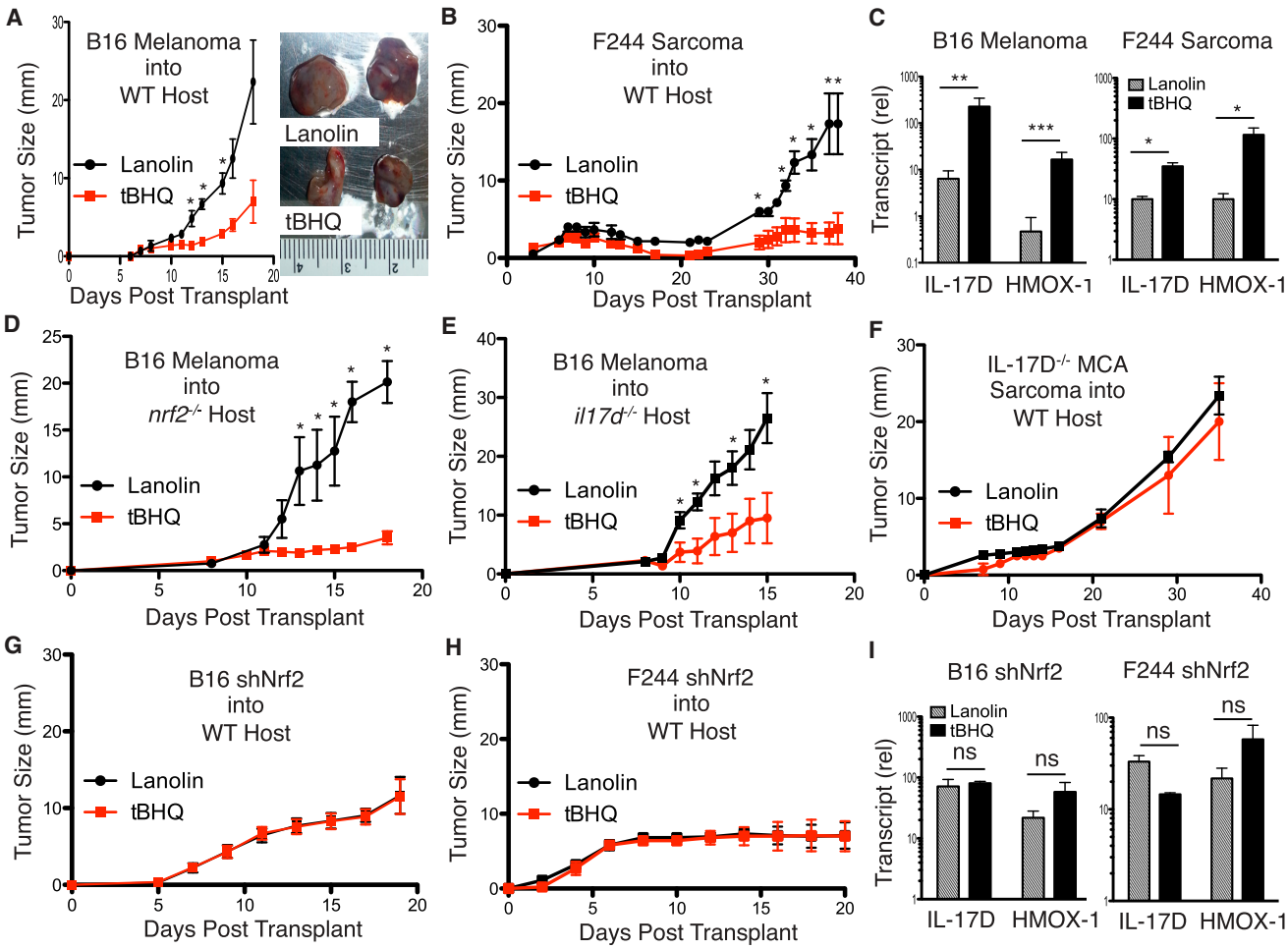

Figure 5. Activating Nrf2 Induces IL-17D and Delays Tumor Growth In Vivo

Tumor cells were transplanted subcutaneously and allowed to reach an established size (~3 × 3 mm) before the initiation of topical treatments with tBHQ once daily for 7 days.

(A and B) When transplanted in WT hosts, B16 (A) and F244 (B) regress following tBHQ treatment.

(C) *Il17d* and the Nrf2 target gene *hmox1* are upregulated in B16 and F244 tumors treated with tBHQ.

(D and E) Topical treatments with tBHQ delay the growth of B16 when transplanted into *nrf2*$^{-/-}$ (D) and *il17d*$^{-/-}$ (E) mice.

(F) Topical tBHQ fails to induce the regression of *il17d*$^{-/-}$ MCA sarcoma cells transplanted into WT mice.

(G and H) tBHQ treatment fails to delay tumor growth when *nrf2* is knocked down via shRNA in B16 melanoma (G) or F244 sarcoma cells (H).

(I) *Il17d* and the Nrf2 target gene *hmox1* are not induced in B16 and F244 tumors treated with tBHQ after *nrf2* knockdown.

Experiments repeated at least twice with no fewer than ten mice. Error bars represent ± SEM. See also Figure S5.

cancer, we used the *Z* scores from RNA sequencing (RNA-seq) of four NK-cell-expressed genes from TCGA to approximate the presence of NK cells in human skin cutaneous melanoma and sarcoma (Figure S6A). We found no positive correlation, probably due to the fact that TCGA data represent chronic rather than acute induction of IL-17D as assessed in our mouse model. The same held true for the correlation of *il17d* with NK- and macrophage-recruiting gene products (CCL5 and CCL2, Figures S6B and S6C) as well as NK cell-expressed genes NKG2D and NKP46 (Figures S6D and S6E). This does not exclude a role for Nrf2 and IL-17D in NK cell recruitment in human cancers, but rather calls for a more detailed analysis of human cancer biopsies after acute induction of IL-17D. To date, this is not possible but might be done in the future if tBHQ or another Nrf2 agonist reaches clinical trials.

DISCUSSION

In this study, we have demonstrated an obligate role for IL-17D in effective tumor surveillance, optimal antiviral responses, and cancer immune therapy via Nrf2 agonists. It is well established that immune responses to viruses and transformed cells have overlapping features (Raulet and Guerra, 2009): both involve NK cells, Th1 immunity, and CD8^{+} T cells. Moreover, NKG2D ligands are induced by viral infection (Shafi et al., 2011; Vivier et al., 2011) as well as being constitutively expressed on cancer

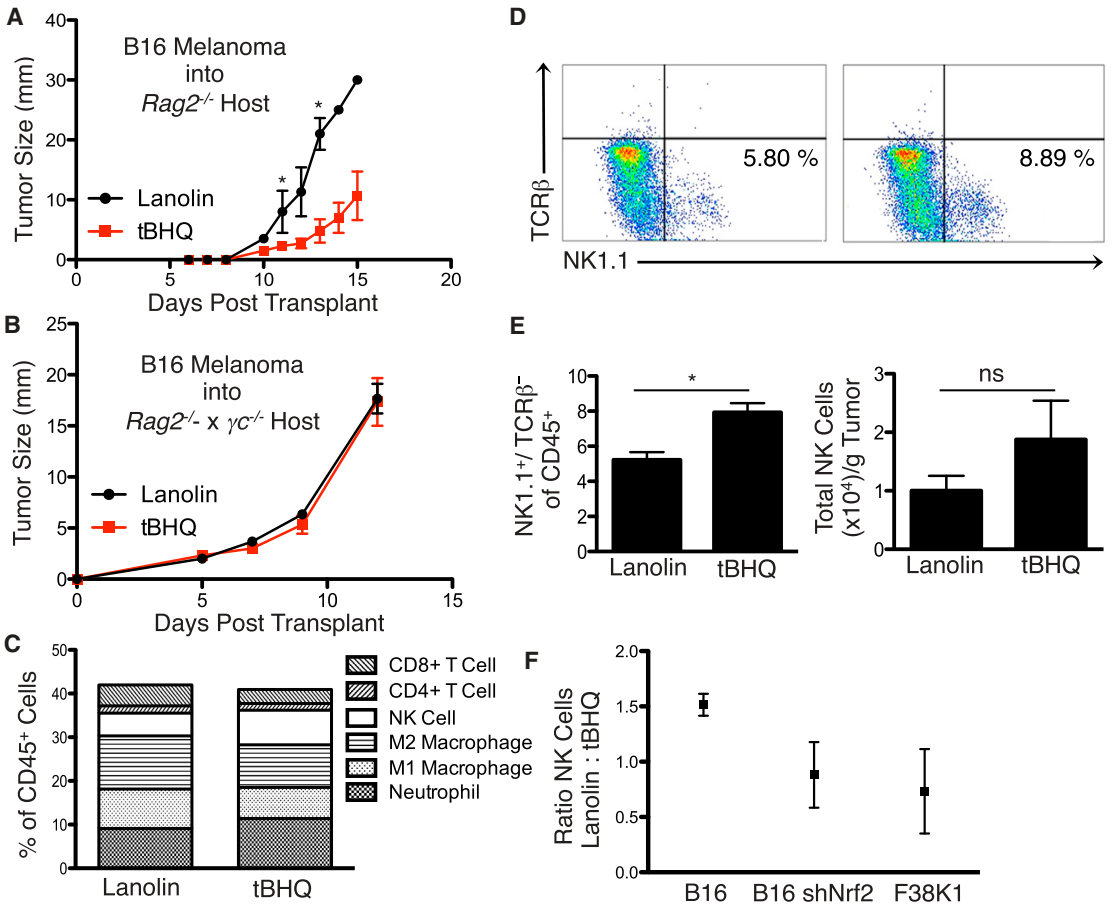

Figure 6. Inducing Nrf2 via tBHQ Leads to the Recruitment of NK Cells into Tumors

(A and B) tBHQ delays the growth of B16 tumors when transplanted into *Rag2*$^{-/-}$ (A) but not *Rag2*$^{-/-}$x $\gamma c^{-/-}$ (B) hosts.

(C–E) Topical treatment of B16 melanomas with tBHQ increases the percentage (C–E) and total number (E) of NK cells present in tumors, while other immune populations remain unchanged (C).

(F) The tBHQ-induced increase in NK cell recruitment is prevented when *nrf2* is knocked down or *il17d* is deleted (F38K1) in tumors.

Experiments repeated at least twice. Error bars represent ± SEM. See also Figures S4–S6.

cells (Diefenbach et al., 2001; Guerra et al., 2008). As such, our finding that IL-17D is induced by viral infection and expressed constitutively by immunogenic cancer cells has precedence in principle and data.

We have definitively shown that Nrf2, an oxidative stress response factor, can function as a tumor suppressor via direct induction of IL-17D. A tumor suppressor role for Nrf2 is supported by previous studies showing that mice genetically deficient in Nrf2 are more susceptible to a wide range of carcinogen-induced cancers (for review, see Ma and He, 2012). For example, *nrf2*$^{-/-}$ mice displayed increased incidence of forestomach cancer (Ramos-Gomez et al., 2003) and bladder cancer (Iida et al., 2004) induced by carcinogens known to induce oxidative stress. *Nrf2*$^{-/-}$ mice also had increased skin cancer in a model of sulforaphane-mediated protection from DMBA/TPA induced carcinogenesis (Xu et al., 2006). There are no studies to address whether Nrf2 participates in tumor immunosurveillance in any of these model systems. Importantly, cancer immunoediting and tumor elimination have been extensively documented in mouse models of MCA-induced sarcomas, and it was recently shown that MCA can acutely induce Nrf2 and its target genes in liver after 24 hr (Jin and Dong, 2013). Accordingly, we show that Nrf2, its target genes and IL-17D are induced in MCA tumors. We suggest that Nrf2 can mediate anti-cancer functions by inducing immune-dependent pathways, namely the IL-17D-dependent recruitment of NK cells.

In contrast to the tumor suppressor role of Nrf2, other studies have shown that Nrf2 expression in tumor cells can promote their survival in the face of oxidative stress, hypoxia, and/or chemotherapy (Jaramillo and Zhang, 2013; Sporn and Liby, 2012). In fact, Nrf2 blockade has become an anti-cancer approach since certain cancer cells (and model systems) report oncogene-induced, constitutive Nrf2 activity as associated with tumor growth and metastasis (DeNicola et al., 2011; Shelton and Jaiswal, 2013). These studies have prompted a re-evaluation of the role of Nrf2 in cancer and support a model whereby Nrf2 is a "double-edged sword" that can suppress or promote cancer. Notably, a recent study found that Nrf2 acts early in

tumorigenesis to suppress tumor formation and later-on to promote tumor formation (Satoh et al., 2013). We propose that Nrf2-mediated induction of IL-17D activates antitumor immunity at an early stage to eliminate the tumor before Nrf2 exerts its pro-tumor activity. This early immune pressure mediated by NK cells could lead to cancer immunoediting, resulting in the loss of IL-17D expression as an immune evasion mechanism. Therefore, the expression of IL-17D in late stage human cancers may not always correlate with good prognosis or NK cell infiltration, as shown in Table S2 and Figures S2B, S2C, and S6. In fact, given the known tumor promoting roles of Nrf2, late stage human cancers that display chronic inflammation may express high levels of Nrf2 without incurring the antitumor responses that could be mediated by IL-17D and/or NK cells. Thus, it will be important to determine if acute induction of Nrf2 in human cancer can indeed serve as a therapeutic mechanism to induce IL-17D and/or recruit NK cells to mediate antitumor immune responses.

We have implicated that Nrf2 agonists, some of which are currently in clinical trials, would be highly efficacious inducers of cancer immunosurveillance and immune therapy by acutely inducing IL-17D. Further studies are needed to determine whether Nrf2 agonists can be used to treat a broad range of established human tumors and/or prevent the development of cancer. It will be important to cast a broad and deep net in these studies, as it is likely that the role of the Nrf2-IL-17D pathway in tumor progression is context-dependent. Notably, our data suggest that the clinical use of antioxidants to prevent cancer and promote overall health may inadvertently limit Nrf2 induction and attenuate an endogenous tumor surveillance pathway. On the other hand, judicious use of oxidative species may find a niche in immunotherapy. For example, drugs such as tBHQ, which do not induce ROS but can directly induce the Nrf2-IL-17D pathway may have even higher efficacy as they would activate an endogenous tumor surveillance pathway without producing genotoxic ROS.

The role of other IL-17 family members in cancer is still controversial. For the most studied member, IL-17A, tumor-promoting roles (Charles et al., 2009; Nam et al., 2008; Numasaki et al., 2003), antitumor functions (Benatar et al., 2008; Benchetrit et al., 2002; Muranski et al., 2008), and immune cell recruiting roles (Martin-Orozco et al., 2009) have all been documented. Specifically, an antitumor role in humans was shown whereby IL-17A production correlated with $CD8^+$ T cell and $CD57^+$ NK cell presence in esophageal squamous cell carcinomas (Lv et al., 2011) and was associated with the induction of T cell-, NK cell- and DC-attracting chemokines (Lu et al., 2013). On the other hand, a pro-tumor role for IL-17A was shown in breast cancer whereby neutralizing IL-17A with antibodies reduced chemokine expression and thereby breast cancer cell migration and metastasis (Roy et al., 2014). Although we have only defined antitumor activities for IL-17D, the fact that Nrf2 can induce IL-17D might suggest that IL-17D could also have tumor promoting activities, similar to IL-17A. This could certainly limit therapies based on IL-17D.

We also found that IL-17D is induced by viral infection and is required for optimal antiviral responses. The IL-17 family of cytokines has been characterized as essential to antimicrobial host defense (for reviews, see Gaffen, 2011; Gu et al., 2013; Iwakura et al., 2011; Jin and Dong, 2013). Specifically, IL-17C and IL-17A/F are thought to mediate anti-bacterial and anti-fungal responses via recruitment of neutrophils. IL-17E contributes to anti-helminth responses via recruitment of eosinophils. Our finding that IL-17D is induced during viral infection, recruits NK cells, and is required for optimal responses to VV and MCMV infection, suggests that the IL-17 family may have evolved to mediate distinct and specific anti-pathogen responses. Given the ancient origin of the IL-17 family, it is tempting to speculate that IL-17D and IL-17C were the first family members to evolve to mediate local control of pathogen infection prior to the evolution of adaptive immunity.

To date, the signals that induce and maintain Nrf2 activity during carcinogenesis are still unclear. We speculate that during tumor formation, Nrf2 activation occurs acutely due to carcinogen exposure, is maintained subacutely by oncogenes, and can be detected constitutively in advanced cancers by mutation or inflammatory cells providing an oxidative burst. Indeed, previous studies have found that MCA induced Nrf2 and its target genes acutely (Jin et al., 2014), in line with our finding that MCA induced Nrf2 and IL-17D in our tumor model. Moreover, oncogenic alleles have been shown to induce Nrf2 (DeNicola et al., 2011), and mutations in KEAP1 can be detected in cancer cells, leading to constitutive Nrf2 activation (Padmanabhan et al., 2006; Shibata et al., 2008; Sjöblom et al., 2006). Future studies will clarify the kinetics of Nrf2 and IL-17D induction during tumor formation.

Finally, it is clear that cancers display metabolic and oxidative stress while also demonstrating an inflammatory component. In fact, these characteristics of cancer have been touted as "next generation hallmarks" (Hanahan and Weinberg, 2011). Based on our findings, it is tempting to conclude that the Nrf2/IL-17D pathway represents an important molecular bridge that connects two hallmarks of cancer—inflammation and oxidative stress.

EXPERIMENTAL PROCEDURES

Transcription Factor Binding Analysis

Sequences for mouse and human *il17d* genes were analyzed for the presence of antioxidant responsive elements (ARE) (5′-TGAcTCAGCa-3′), a sequence to which the Nrf2-sMAF heterodimer is known to bind (Nguyen et al., 2003). ARE sequences identified in mouse and human *il17d* genes are listed in Table S1.

Cell Lines

MCA-induced sarcoma cell lines were generated from primary tumors and expanded in vitro until at least the second passage before freezing. For experimentation, tumor cell lines were thawed from early passages and grown in RPMI 1640 (GIBCO) supplemented with 10% FCS (Atlanta Biologics) as previously described (O'Sullivan et al., 2012). Other tumor cell lines used—Ramos, B16, LLC—were cultured similarly. Primary-derived mouse embryonic fibroblasts were derived from fetuses 12.5–13.5 days p.c. (as described in Conner, 2001a, 2001b).

Nrf2 Activation and Knockdown

Nrf2 was activated in cell lines in vitro with either *tert*-butylhydroquinone (Spectrum) or H_2O_2 (Fisher). tBHQ was used at 50 μM in DMSO, and H_2O_2 was used at 10 μM for 0.5–1 hr before being washed out. Treated cells were harvested at time points between 6 and 12 hr for analysis. Activation of Nrf2 in vivo was adapted from methods described by (Schäfer et al., 2014). For in vivo Nrf2 activation, a cream containing 50mM tBHQ solubilized in DMSO was mixed 1:1 (v/v) with Lanolin cream (Sigma) (controls were a 1:1 mixture

of DMSO:lanolin) and heated gently in a water bath to allow for mixing. The mixture was allowed to cool overnight before use. Hair along the flank was removed one day before the initiation of topical treatments. To knock down Nrf2, a mixture of three siRNAs to *nrf2* or control siRNA were used (Invitrogen) (Fujita et al., 2011). siRNA was transfected into cells with Lipofectamine 2000 (Thermo Fisher) as recommended by the manufacturer. For shRNA knockdown, five different shRNAs to *nrf2* or control shRNA (Sigma) were co-transfected with lentiviral plasmids into 293T cells using Lipofectamine 2000. Virus-containing supernatant was used to transduce sarcoma and melanoma tumor cell lines. Cells were grown in the presence of 10-40 μg/ml puromycin, and *nrf2* knockdown was confirmed with qPCR.

The Cancer Genome Atlas

Human tumor data were sourced from the TCGA analytical tool, UCSC Cancer Genome Browser (http://cancergenome.nih.gov/). PANCAN normalized gene expression data were used to partition tumors into roughly equally numbered groups, compare transcript expression levels, and generate survival curves for patients. For ARE-containing gene signature, the following genes were used: *hmox1*, *NADPH dehydrogenase* (*nqo*)*1*, *thioredoxin reductase* (*txnrd*)*1*, *glutathione S-transferase-alpha* (*gsta*)*4*, *-mu* (*gstm*) *1 and 3*, *sulfiredoxin* (*srxn*) *1*, *epoxide hydrolase* (*ephx*)*1*, and *alsin Rho guanine nucleotide exchange factor* (*als*)*2*. For analyzing NK cell metagenes, the expression *Z* scores from RNA-seq for the genes *perforin1*, *granzyme B*, *NKG2D*, and *natural cytotoxicity triggering receptor1* were added up and used as "NK score" (approximation of the presence of NK cells).

Mice

C57BL/6-strain WT, C57BL/6 ×129-strain WT, B6-*Rag2*$^{tm1.1Cgn}$ (*rag2*$^{-/-}$), B6-*Rag2*^{tm1Fwa} *Il2rγ*^{tm1Wjl} (*rag2*$^{-/-}$ *γc*$^{-/-}$), B6-*Il17d*^{tm1Lex}/Mmucd (*il17d*$^{-/-}$) (UC Davis MMRC), and B6-*Nfe2l2*^{tm1Ywk}/J (*nrf2*$^{-/-}$) (Jackson) were used for studies in this work. To control for microbiota-influenced immunity disparities, WT mice were bred for at least one generation in house before use. *Rag2*$^{-/-}$ and *Rag2*$^{-/-}$ *γc*$^{-/-}$ colonies are maintained and in routine use in our lab. *Il17d*$^{-/-}$ and *nrf2*$^{-/-}$ mice were obtained from UC Davis MMRC and Jackson Laboratory, respectively. Mice were backcrossed to a C57/Bl6 background for several generations until >99% pure. All mouse experiments were approved by the University of California, San Diego (UCSD) Institutional Animal Care and Use Committee (IACUC protocol #S06201) using a marker assisted selection (i.e., "speed congenic") approach. Mouse genomes were assessed at the DartMouse Speed Congenic Core Facility at the Geisel School of Medicine at Dartmouth. DartMouse uses the Illumina GoldenGate Genotyping Assay to interrogate 1449 SNPs spread throughout the genome. The raw SNP data were analyzed using DartMouse's SNaP-Map and Map-Synth software, allowing the determination for each mouse of the genetic background at each SNP location. Genetic background at the final backcross generation was determined to be >99% for the desired C57BL/6 background. *nrf2* genotyping was performed as recommended (Jackson Laboratory), and *il17d* genotypes from tail biopsies were determined using real-time PCR (Transnetyx).

Tumorigenesis and Tumor Transplantations

Primary tumorigenesis was performed as previously described (O'Sullivan et al., 2012; Shankaran et al., 2001). MCA was dissolved in corn oil (Sigma) prior to instillation. To induce primary tumors, 5-μg or 25-μg doses of MCA were injected subcutaneously along a single flank. Tumor development was monitored and measured weekly between 2 and 6 months post MCA instillation. Tumors were harvested for cell line generation and RNA when tumors achieved an average diameter of 25 mm. For transplantation studies, tumor cell lines were trypsinized, washed with cold PBS three times, and injected subcutaneously along the flanks of mice (previously described in O'Sullivan et al., 2012). Hair was removed from the flanks of mice at least 1 day prior to transplantation. Tumor progression was assessed by averaging the greatest two diameter measurements of the tumor.

Viral Infections

VV Western Reserve was kindly donated by the Dr. Ananda Goldrath (UCSD) and MCMV Smith Strain by Dr. Elina Zuniga (UCSD). Primary fibroblasts or tumor cell lines were incubated with 1 × 10^5 pfu of MCMV or VV, respectively, per 4 × 10^5 cells for 2 hr, washed and harvested after 24 hr. Viral titers following VV infection were determined by plaque assays on Vero cells (kindly donated by Dr. Elina Zuniga). In vivo, age- and sex-matched 8- to 12-week-old C57Bl/6 WT or *il17d*$^{-/-}$ mice were infected with VV by scarification at 1 × 10^5 or 1 × 10^6 pfu. VV scars were monitored daily and expressed as the average of the two maximum scar diameters. For MCMV, mice were infected with 3 × 10^5 pfu/mouse intraperitoneally (i.p.) and weighed daily for disease progression.

Antibodies and FACS Analysis

Tumor tissues were digested both mechanically by chopping with razor blades and chemically with 1 mg/ml type IA collagenase (Sigma-Aldrich) for 30 min at 37°C. Following digestion, cell suspensions were washed, filtered, and stained as previously described (O'Sullivan et al., 2012). The following antibodies were used: Ly6C (ER-MP20, Serotec), MHCII (M5/114 15.2, eBioscience), Ly6G (1A8, Biolegend), CD8 (53-6.7, eBioscience), CD44 (IM7, Biolegend), CD3 (17A.2, Biolegend), CD4 (GK1.5, Biolegend), CD69 (H1.2F3, Biolegend), Granzyme B (NGZB, eBioscience), IFNγ (XMG 1.2, Biolegend), TCRβ (H57-597, Biolegend), B220 (RA3-6B2, eBioscience), NK1.1 (PK136, Biolegend), CD11b (M1/70, eBioscience), and CD45 (30-F11, Biolegend). Stained cell suspensions were analyzed on a BD FACS CANTO II (BD Biosciences).

Western Blot

Cells were lysed in 4× sample buffer containing SDS (Bio-Rad) and β-mercaptoethanol (Sigma) before boiling at 95°C for 5 min. Samples were run on SDS-PAGE gels (Bio-Rad), and expression of Nrf2 was analyzed by western blotting using anti-Nrf2 (C-20, Santa Cruz Biotech). β-actin (A5441, Sigma-Aldrich) was used as loading control. Blotted bands were quantified with CS6 Photoshop imaging software.

Immunohistochemistry

Tissues were fixed in 10% formalin (Sigma-Aldrich) for 24 hr before embedding in paraffin. Sections were stained with α-Nrf2 (C-20) by the UCSD Core Histology and Immunohistochemistry service using the Ventana Discovery Ultra (Roche). Slides were imaged on a Leica DM 2500 microscope and photographed with a Leica DFC 420 digital camera.

Chromatin Immunoprecipitation

ChIP for Nrf2 was performed as described previously (DeNicola et al., 2011). Following activation of Nrf2 with tBHQ, cells were fixed in 1% formaldehyde for 10 min at room temperature, quenched with 0.125 M glycine for 5 min at room temperature, washed with cold PBS, and resuspended in lysis buffer (1% SDS, 10 mM EDTA [pH 8], 50 mM Tris-HCL[pH 8]), fresh protease inhibitor cocktail for 5 min on ice. To generate chromatin fragments of ~200 bp, cell lysates were sonicated on ice for 15 cycles (15-s on, 45-s off) and pelleted by centrifugation at 13,000 rpm for 5 min. Protein A Dynabeads (Life Technologies), pre-blocked in 0.5% BSA in PBS (w/v), were incubated with 8 μg α-Nrf2 (C-20) or normal rabbit IgG (sc-2027, Santa Cruz Biotech) overnight at 4°C and then washed with additional blocking buffer and RIPA. To immunoprecipitate Nrf2-chromatin complexes, conjugated Dynabeads were mixed with sonicated lysate—diluted 1:9 in dilution buffer with protease inhibitors—and allowed to rotate overnight at 4°C. Immunoprecipitates were processed as suggested by the Dynabeads manufacturer (Life Technologies) and purified using the QiaQuick PCR DNA kit (QIAGEN). qPCR sequences used for ChIP samples appear in Table S3.

qPCR

RNA was isolated with Trizol (Ambion) and converted to cDNA (Applied Biosystems High-Capacity cDNA Reverse Transcription Kit). qPCRs were prepared with 2× Universal SYBR Green Master Mix (Applied Biosystems) and performed on Bio-Rad CFX96 (Bio-Rad) machine. The following primer sequences were used: HPRT (forward: 5′-GCTTGCTGGTGAAAAGGACC TCTCGAAG-3′; reverse: 5′-CCCTGAAGTACTCATTATAGTCAAGGGCAT-3′), IL-17D (forward: 5′-AGCTTGTCCATGCTGGAGTT-3′; reverse: 5′-CTCTACG GGGAGGAGGACTT-3′), HMOX-1 (forward: 5′-TGAAGGAGGCCACCAAGG AGG-3′; reverse: 5′-AGAGGTCACCCAGGTAGCGGG-3′), and Keratin 18 (forward: 5′-AGCCATTACTTCAAGATCATC-3′; reverse: 5′-CTCTGTCTCATAC TTGACTCT-3′).

Statistical Analysis

Statistical significance was determined by the Welch's t test, using a two-tailed analysis, the log-rank test, or the repeated-measures ANOVA test with the InStat 3.0 software (GraphPad). Error bars are depicted using SEM. All experiments were repeated at least twice (*$p < 0.05$, **$p < 0.01$, ***$p < 0.001$ in all data shown).

SUPPLEMENTAL INFORMATION

Supplemental Information includes six figures and three tables and can be found with this article online at http://dx.doi.org/10.1016/j.celrep.2016.07.075.

AUTHOR CONTRIBUTIONS

R.S.-K., R.S., and J.D.B. designed the experiments. R.S.-K., R.S., E.T.E.G., S.C.S., A.W., Jr., E.K.S., B.L., and T.E.O'S. performed and analyzed the experiments. E.L. and O.H. contributed analytical tools. J.D.B. supervised the research. R.S.-K., R.S., and J.D.B. wrote the paper.

ACKNOWLEDGMENTS

J.D.B. is supported by grants from the NCI (CA157885) and The Hartwell Foundation. O.H. is supported by a grant from the NCI (CA177519). R.S. is supported by the DFG (SE 2418/1-1).

Received: April 6, 2015
Revised: June 8, 2016
Accepted: July 27, 2016
Published: August 18, 2016

REFERENCES

Aran, D., Sirota, M., and Butte, A.J. (2015). Systematic pan-cancer analysis of tumour purity. Nat. Commun. *6*, 8971.

Benatar, T., Cao, M.Y., Lee, Y., Li, H., Feng, N., Gu, X., Lee, V., Jin, H., Wang, M., Der, S., et al. (2008). Virulizin induces production of IL-17E to enhance antitumor activity by recruitment of eosinophils into tumors. Cancer Immunol. Immunother. *57*, 1757–1769.

Benchetrit, F., Ciree, A., Vives, V., Warnier, G., Gey, A., Sautès-Fridman, C., Fossiez, F., Haicheur, N., Fridman, W.H., and Tartour, E. (2002). Interleukin-17 inhibits tumor cell growth by means of a T-cell-dependent mechanism. Blood *99*, 2114–2121.

Charles, K.A., Kulbe, H., Soper, R., Escorcio-Correia, M., Lawrence, T., Schultheis, A., Chakravarty, P., Thompson, R.G., Kollias, G., Smyth, J.F., et al. (2009). The tumor-promoting actions of TNF-alpha involve TNFR1 and IL-17 in ovarian cancer in mice and humans. J. Clin. Invest. *119*, 3011–3023.

Conner, D.A. (2001a). Mouse embryonic stem (ES) cell culture. Curr. Protoc. Mol. Biol. *Chapter 23*, Unit 23.3.

Conner, D.A. (2001b). Mouse embryonic stem (ES) cell isolation. Curr. Protoc. Mol. Biol. *Chapter 23*, Unit 23.4.

DeNicola, G.M., Karreth, F.A., Humpton, T.J., Gopinathan, A., Wei, C., Frese, K., Mangal, D., Yu, K.H., Yeo, C.J., Calhoun, E.S., et al. (2011). Oncogene-induced Nrf2 transcription promotes ROS detoxification and tumorigenesis. Nature *475*, 106–109.

Diefenbach, A., Jensen, E.R., Jamieson, A.M., and Raulet, D.H. (2001). Rae1 and H60 ligands of the NKG2D receptor stimulate tumour immunity. Nature *413*, 165–171.

Fujita, K., Maeda, D., Xiao, Q., and Srinivasula, S.M. (2011). Nrf2-mediated induction of p62 controls Toll-like receptor-4-driven aggresome-like induced structure formation and autophagic degradation. Proc. Natl. Acad. Sci. USA *108*, 1427–1432.

Gaffen, S.L. (2011). Recent advances in the IL-17 cytokine family. Curr. Opin. Immunol. *23*, 613–619.

Gorrini, C., Harris, I.S., and Mak, T.W. (2013). Modulation of oxidative stress as an anticancer strategy. Nat. Rev. Drug Discov. *12*, 931–947.

Gu, C., Wu, L., and Li, X. (2013). IL-17 family: cytokines, receptors and signaling. Cytokine *64*, 477–485.

Guerra, N., Tan, Y.X., Joncker, N.T., Choy, A., Gallardo, F., Xiong, N., Knoblaugh, S., Cado, D., Greenberg, N.M., and Raulet, D.H. (2008). NKG2D-deficient mice are defective in tumor surveillance in models of spontaneous malignancy. Immunity *28*, 571–580.

Hanahan, D., and Weinberg, R.A. (2011). Hallmarks of cancer: the next generation. Cell *144*, 646–674.

Iida, K., Itoh, K., Kumagai, Y., Oyasu, R., Hattori, K., Kawai, K., Shimazui, T., Akaza, H., and Yamamoto, M. (2004). Nrf2 is essential for the chemopreventive efficacy of oltipraz against urinary bladder carcinogenesis. Cancer Res. *64*, 6424–6431.

Iwakura, Y., Ishigame, H., Saijo, S., and Nakae, S. (2011). Functional specialization of interleukin-17 family members. Immunity *34*, 149–162.

Jaramillo, M.C., and Zhang, D.D. (2013). The emerging role of the Nrf2-Keap1 signaling pathway in cancer. Genes Dev. *27*, 2179–2191.

Jin, W., and Dong, C. (2013). IL-17 cytokines in immunity and inflammation. Emerg. Microbes Infect. *2*, e60.

Jin, Y., Miao, W., Lin, X., Pan, X., Ye, Y., Xu, M., and Fu, Z. (2014). Acute exposure to 3-methylcholanthrene induces hepatic oxidative stress via activation of the Nrf2/ARE signaling pathway in mice. Environ. Toxicol. *29*, 1399–1408.

Kensler, T.W., and Wakabayashi, N. (2010). Nrf2: friend or foe for chemoprevention? Carcinogenesis *31*, 90–99.

Lu, L., Pan, K., Zheng, H.X., Li, J.J., Qiu, H.J., Zhao, J.J., Weng, D.S., Pan, Q.Z., Wang, D.D., Jiang, S.S., et al. (2013). IL-17A promotes immune cell recruitment in human esophageal cancers and the infiltrating dendritic cells represent a positive prognostic marker for patient survival. J. Immunother. *36*, 451–458.

Lv, L., Pan, K., Li, X.D., She, K.L., Zhao, J.J., Wang, W., Chen, J.G., Chen, Y.B., Yun, J.P., and Xia, J.C. (2011). The accumulation and prognosis value of tumor infiltrating IL-17 producing cells in esophageal squamous cell carcinoma. PLoS ONE *6*, e18219.

Ma, Q. (2013). Role of nrf2 in oxidative stress and toxicity. Annu. Rev. Pharmacol. Toxicol. *53*, 401–426.

Ma, Q., and He, X. (2012). Molecular basis of electrophilic and oxidative defense: promises and perils of Nrf2. Pharmacol. Rev. *64*, 1055–1081.

Malhotra, D., Portales-Casamar, E., Singh, A., Srivastava, S., Arenillas, D., Happel, C., Shyr, C., Wakabayashi, N., Kensler, T.W., Wasserman, W.W., and Biswal, S. (2010). Global mapping of binding sites for Nrf2 identifies novel targets in cell survival response through ChIP-Seq profiling and network analysis. Nucleic Acids Res. *38*, 5718–5734.

Martin-Orozco, N., Muranski, P., Chung, Y., Yang, X.O., Yamazaki, T., Lu, S., Hwu, P., Restifo, N.P., Overwijk, W.W., and Dong, C. (2009). T helper 17 cells promote cytotoxic T cell activation in tumor immunity. Immunity *31*, 787–798.

Martindale, J.L., and Holbrook, N.J. (2002). Cellular response to oxidative stress: signaling for suicide and survival. J. Cell. Physiol. *192*, 1–15.

Mazurier, F., Fontanellas, A., Salesse, S., Taine, L., Landriau, S., Moreau-Gaudry, F., Reiffers, J., Peault, B., Di Santo, J.P., and de Verneuil, H. (1999). A novel immunodeficient mouse model–RAG2 x common cytokine receptor gamma chain double mutants–requiring exogenous cytokine administration for human hematopoietic stem cell engraftment. J. Interferon Cytokine Res. *19*, 533–541.

Muranski, P., Boni, A., Antony, P.A., Cassard, L., Irvine, K.R., Kaiser, A., Paulos, C.M., Palmer, D.C., Touloukian, C.E., Ptak, K., et al. (2008). Tumor-specific Th17-polarized cells eradicate large established melanoma. Blood *112*, 362–373.

Nam, J.S., Terabe, M., Kang, M.J., Chae, H., Voong, N., Yang, Y.A., Laurence, A., Michalowska, A., Mamura, M., Lonning, S., et al. (2008). Transforming growth factor beta subverts the immune system into directly promoting tumor growth through interleukin-17. Cancer Res. *68*, 3915–3923.

Nguyen, T., Sherratt, P.J., and Pickett, C.B. (2003). Regulatory mechanisms controlling gene expression mediated by the antioxidant response element. Annu. Rev. Pharmacol. Toxicol. *43*, 233–260.

Numasaki, M., Fukushi, J., Ono, M., Narula, S.K., Zavodny, P.J., Kudo, T., Robbins, P.D., Tahara, H., and Lotze, M.T. (2003). Interleukin-17 promotes angiogenesis and tumor growth. Blood *101*, 2620–2627.

O'Sullivan, T., Saddawi-Konefka, R., Vermi, W., Koebel, C.M., Arthur, C., White, J.M., Uppaluri, R., Andrews, D.M., Ngiow, S.F., Teng, M.W., et al. (2012). Cancer immunoediting by the innate immune system in the absence of adaptive immunity. J. Exp. Med. *209*, 1869–1882.

O'Sullivan, T., Saddawi-Konefka, R., Gross, E., Tran, M., Mayfield, S.P., Ikeda, H., and Bui, J.D. (2014). Interleukin-17D mediates tumor rejection through recruitment of natural killer cells. Cell Rep. *7*, 989–998.

Padmanabhan, B., Tong, K.I., Ohta, T., Nakamura, Y., Scharlock, M., Ohtsuji, M., Kang, M.I., Kobayashi, A., Yokoyama, S., and Yamamoto, M. (2006). Structural basis for defects of Keap1 activity provoked by its point mutations in lung cancer. Mol. Cell *21*, 689–700.

Pergola, P.E., Raskin, P., Toto, R.D., Meyer, C.J., Huff, J.W., Grossman, E.B., Krauth, M., Ruiz, S., Audhya, P., Christ-Schmidt, H., et al.; BEAM Study Investigators (2011). Bardoxolone methyl and kidney function in CKD with type 2 diabetes. N. Engl. J. Med. *365*, 327–336.

Ramos-Gomez, M., Dolan, P.M., Itoh, K., Yamamoto, M., and Kensler, T.W. (2003). Interactive effects of nrf2 genotype and oltipraz on benzo[a]pyrene-DNA adducts and tumor yield in mice. Carcinogenesis *24*, 461–467.

Raulet, D.H., and Guerra, N. (2009). Oncogenic stress sensed by the immune system: role of natural killer cell receptors. Nat. Rev. Immunol. *9*, 568–580.

Roy, L.D., Sahraei, M., Schettini, J.L., Gruber, H.E., Besmer, D.M., and Mukherjee, P. (2014). Systemic neutralization of IL-17A significantly reduces breast cancer associated metastasis in arthritic mice by reducing CXCL12/SDF-1 expression in the metastatic niches. BMC Cancer *14*, 225.

Saddawi-Konefka, R., O'Sullivan, T., Gross, E.T., Washington, A., Jr., and Bui, J.D. (2015). Tumor-expressed IL-17D recruits NK cells to reject tumors. OncoImmunology *3*, e954853.

Satoh, H., Moriguchi, T., Takai, J., Ebina, M., and Yamamoto, M. (2013). Nrf2 prevents initiation but accelerates progression through the Kras signaling pathway during lung carcinogenesis. Cancer Res. *73*, 4158–4168.

Schäfer, M., Farwanah, H., Willrodt, A.H., Huebner, A.J., Sandhoff, K., Roop, D., Hohl, D., Bloch, W., and Werner, S. (2012). Nrf2 links epidermal barrier function with antioxidant defense. EMBO Mol. Med. *4*, 364–379.

Schäfer, M., Willrodt, A.H., Kurinna, S., Link, A.S., Farwanah, H., Geusau, A., Gruber, F., Sorg, O., Huebner, A.J., Roop, D.R., et al. (2014). Activation of Nrf2 in keratinocytes causes chloracne (MADISH)-like skin disease in mice. EMBO Mol. Med. *6*, 442–457.

Schwarz, K.B. (1996). Oxidative stress during viral infection: a review. Free Radic. Biol. Med. *21*, 641–649.

Shafi, S., Vantourout, P., Wallace, G., Antoun, A., Vaughan, R., Stanford, M., and Hayday, A. (2011). An NKG2D-mediated human lymphoid stress surveillance response with high interindividual variation. Sci. Transl. Med. *3*, 113ra124.

Shankaran, V., Ikeda, H., Bruce, A.T., White, J.M., Swanson, P.E., Old, L.J., and Schreiber, R.D. (2001). IFNgamma and lymphocytes prevent primary tumour development and shape tumour immunogenicity. Nature *410*, 1107–1111.

Shelton, P., and Jaiswal, A.K. (2013). The transcription factor NF-E2-related factor 2 (Nrf2): a protooncogene? FASEB J. *27*, 414–423.

Shibata, T., Kokubu, A., Gotoh, M., Ojima, H., Ohta, T., Yamamoto, M., and Hirohashi, S. (2008). Genetic alteration of Keap1 confers constitutive Nrf2 activation and resistance to chemotherapy in gallbladder cancer. Gastroenterology *135*, 1358–1368.

Shinkai, Y., Rathbun, G., Lam, K.P., Oltz, E.M., Stewart, V., Mendelsohn, M., Charron, J., Datta, M., Young, F., Stall, A.M., et al. (1992). RAG-2-deficient mice lack mature lymphocytes owing to inability to initiate V(D)J rearrangement. Cell *68*, 855–867.

Sjöblom, T., Jones, S., Wood, L.D., Parsons, D.W., Lin, J., Barber, T.D., Mandelker, D., Leary, R.J., Ptak, J., Silliman, N., et al. (2006). The consensus coding sequences of human breast and colorectal cancers. Science *314*, 268–274.

Sporn, M.B., and Liby, K.T. (2012). NRF2 and cancer: the good, the bad and the importance of context. Nat. Rev. Cancer *12*, 564–571.

Tkachev, V.O., Menshchikova, E.B., and Zenkov, N.K. (2011). Mechanism of the Nrf2/Keap1/ARE signaling system. Biochemistry (Mosc.) *76*, 407–422.

Türei, D., Papp, D., Fazekas, D., Földvári-Nagy, L., Módos, D., Lenti, K., Csermely, P., and Korcsmáros, T. (2013). NRF2-ome: an integrated web resource to discover protein interaction and regulatory networks of NRF2. Oxid. Med. Cell. Longev. *2013*, 737591.

Vivier, E., Raulet, D.H., Moretta, A., Caligiuri, M.A., Zitvogel, L., Lanier, L.L., Yokoyama, W.M., and Ugolini, S. (2011). Innate or adaptive immunity? The example of natural killer cells. Science *331*, 44–49.

Xu, C., Huang, M.T., Shen, G., Yuan, X., Lin, W., Khor, T.O., Conney, A.H., and Kong, A.N. (2006). Inhibition of 7,12-dimethylbenz(a)anthracene-induced skin tumorigenesis in C57BL/6 mice by sulforaphane is mediated by nuclear factor E2-related factor 2. Cancer Res. *66*, 8293–8296.